Mode coupling dynamics and communication strategies for multi-core fiber systems

Florence Y. M. Chan,* Alan Pak Tao Lau, and Hwa-Yaw Tam

Department of Electrical Engineering, The Hong Kong Polytechnic University, Hong Kong, China
**fym.chan@yahoo.com*

Abstract: The propagation dynamics of 7-core multi-core fibers (MCFs) with identical and three-types of cores are analytically derived based on the coupled-mode theory. The mode coupling dynamics can be aperiodic with transmission distance for MCF with identical cores. For MCFs with heterogeneous cores, it is found that even though signals from different core groups will not couple with each other, the coupling within their own group is significantly affected by the presence of other core groups. Joint signal processing techniques to mitigate mode coupling induced-cross-talks such as least mean square (LMS) algorithm and maximum likelihood (ML) detection are investigated and corresponding transmission performance are determined for coherent as well as intensity modulated formats. It is shown that aperiodic mode coupling in intensity modulated systems induces cross-talks that are difficult to eliminate through signal processing. The analytical insights may help in optimizing MCF designs and corresponding signal processing techniques for future high capacity MCF transmission systems.

OCIS codes: (060.2280) Fiber design and fabrication; (060.2310) Fiber optics; (060.2400) Fiber properties; (060.2430) Fibers, single-mode; (060.4005) Microstructured fibers.

References and links

1. L. A. B. Windover, J. N. Simom, S. A. Rosenau, K. S. Giboney, G. M. Flower, L. W. Mirkarimi, A. Grot, B. Law, C. K. Lin, A. Tandon, R. W. Gruhlke, H. Xia, G. Rankin, M. R. T. Tan, and D. W. Dolfi, "Parallel optical interconnections > 100 Gb/s," J. Lightwave Technol. **22**, 20055–22063 (2004).
2. B. Zhu, T. F. Taunay, M. F. Yan, J. M. Fini, M. Fishteyn, E. M. Monberg, and F. V. Dimarcello, "Seven-core multicore fiber transmissions for passive optical network," Opt. Express **18**(11), 11117–11122 (2010).
3. F. Yaman, N. Bai, B. Zhu, T. Wang, and G. Li, "Long distance transmission in few-mode fibers," Opt. Express **18**(12), 13250–13257 (2010).
4. E. Ip, A. P. T. Lau, D. J. F. Barros, and J. M. Kahn, "Coherent detection in optical fiber systems," Opt. Express **16**(2), 753–791 (2008).
5. M. Koshiba, K. Saitoh, and Y. Kokubun, "Heterogeneous multicore fibres: proposal and design principle," IEICE Electron. Express **6**(2), 98–103 (2009).
6. C. P. Tsekrekos, A. Martinez, F. M. Huijskens, and A. M. J. Koonen, "Design considerations for transparent mode group diversity multiplexing," IEEE Photon. Technol. Lett. **18**(22), 2359–2361 (2006).
7. Y. Kokubun and M. Koshiba, "Novel multi-core fibers for mode division multiplexing: Proposal and design principle," IEICE Electron. Express **6**(8), 522–528 (2009).
8. K. Imamura, K. Mukasa, and T. Yagi, "Multi-core holey fibers for the long-distance (>100 km) ultra large capacity transmission," OFC 2009, OTuC3 (2009).
9. A. P. T. Lau, L. Xu, and T. Wang, "Performance of receivers and detection algorithms for modal multiplexing in multimode fiber systems," IEEE Photon. Technol. Lett. **19**(14), 1087–1089 (2007).
10. A. Al Amin, A. Li, S. Chen, X. Chen, G. Gao, and W. Shieh, "Dual-LP_{11} mode 4x4 MIMO-OFDM transmission over a two-mode fiber," Opt. Express **19**(17), 16672–16679 (2011).
11. S. Randel, R. Ryf, A. Sierra, P. J. Winzer, A. H. Gnauck, C. A. Bolle, R.-J. Essiambre, D. W. Peckham, A. McCurdy, and R. Lingle, Jr., "6×56-Gb/s mode-division multiplexed transmission over 33-km few-mode fiber enabled by 6×6 MIMO equalization," Opt. Express **19**(17), 16697–16707 (2011).
12. J. M. Fini, B. Zhu, T. F. Taunay, and M. F. Yan, "Bends in the design of low-crosstalk multicore fiber communications links," OECC 2010, 7C2–3 (2010).
13. H. Yang, E. Tangdiongga, S. C. J. Lee, C. Okonkwo, H. P. A. van den Boom, S. Randel, and A. M. J. Koonen, "4.7 Gbit-s transmission over 50m long 1mm diameter multi-core plastic optical fiber," OFC 2010, OWA4 (2010).
14. M. Koshiba, "Recent progress in multi-core fibers for ultralarge-capacity transmission," OECC 2010, 6B1–3 (2010).

#156104 - $15.00 USD Received 10 Oct 2011; revised 20 Dec 2011; accepted 1 Feb 2012; published 9 Feb 2012

15. I. Hartl, H. A. McKay, A. Marcinkevicius, L. Dong, and M. E. Fermann, "Multi-core leakage-channel fibers with up to 26000 μm2 combined effective mode-field area," CLEO 2009, CWD1 (2009).
16. P. Zhou, X. Xu, S. Guo, and Z. Liu, "Analysis on power scalability of multicore fiber laser," IEEE IPGC 2008, 1–3 (2008).
17. N. N. Elkin, A. P. Napartovich, V. N. Troshchieva, and D. V. Vysotsky, "Numerical Modeling of multi-core fiber laser," LFNM 2006, 104–109 (2006).
18. N. Peyghambarian, M. Fallahi, H. Li, L. Li, A. Mafi, M. Mansuripur, J. V. Moloney, R. A. Norwood, D. Panasenko, A. Polynkin, P. Polynkin, T. Qiu, A. Schülzgen, V. L. Temyanko, J. Wu, S. Jiang, A. Chavez, J. Geng, and C. Spiegelberg, "Microstructured and mukllticore fibers and fiber lasers," OFC 2006, OFK3 (2006).
19. P. Glas, M. Naumann, A. Schirrmacher, and Th. Pertsch, "The multicore fiber—a novel design for a diode pumped fiber laser," Opt. Commun. **151**(1-3), 187–195 (1998).
20. N. N. Elkin, A. P. Napartovich, V. N. Troshchieva, and D. V. Vysotsky, "Mode competition in multi-core fiber amplifier," Opt. Commun. **277**(2), 390–396 (2007).
21. K. Takenaga, S. Tanigawa, N. Guan, S. Matsuo, K. Saitoh, and M. Koshiba, "Reduction of crosstalk by quasi-homogeneous solid multi-core fiber," OFC 2010, OWK7 (2010).
22. B. Zhu, T. F. Taunay, M. Fishteyn, X. Liu, S. Chandrasekhar, M. F. Yan, J. M. Fini, E. M. Monberg, and F. V. Dimarcello, "112-Tb/s space-division multiplexed DWDM transmission with 14-b/s/Hz aggregate spectral efficiency over a 76.8-km seven-core fiber," Opt. Express **19**(17), 16665–16671 (2011).
23. K. Tomozawa and Y. Kokubun, "Maximum core capacity of heterogeneous uncoupled multi-core fibers," OECC 2010, 7C2–4 (2010).
24. K.Saitoh, T. Matsui, T. Sakamoto, M. Koshiba, and S. Tomita, "Multi-core hole-assisted fibers for high core density space division multiplexing," OECC 2010, 7C2–1 (2010).
25. K. Imamura, K. Mukasa, and T. Yagi, "Investigation on multi-core fibers with large Aeff and low micro bending loss," OFC 2010, OWK6 (2010).
26. T. Hayashi, T. Nagashima, O. Shimakawa, T. Sasaki, and E. Sasaoka, "Crosstalk variation of multi-core fibre due to fibre bend," ECOC 2010, We.8.F.6 (2010).
27. K. Takenaga, Y. Arakawa, S. Tanigawa, N. Guan, S. Matsuo, K. Saitoh, and M. Koshiba, "Reduction of crosstalk by trench-assisted multi-core fiber," OFC 2011, OWJ4 (2011).
28. N. Kishi, E. Yamashita, and K. Atsuki, "Modal and coupling-field analysis of optical fibers with circularly distributed multiple cores and a central core," J. Lightwave Technol. **4**(8), 991–996 (1986).
29. A. W. Snyder, "Coupled-mode theory for optical fibers," J. Opt. Soc. Am. **62**(11), 1267–1277 (1972).
30. A. W. Snyder and J. D. Love, *Optical Waveguide Theory* (Chapman & Hall, 1983), Chap. 29.
31. H. A. Haus and L. Molter-Orr, "Coupled multiple waveguide systems," IEEE J. Quantum Electron. **19**(5), 840–844 (1983).
32. M. Abramowitz and I. A. Stegun, *Handbook of Mathematical Functions* (Dover, 1972).
33. K. Mukasa, K. Imamura, Y. Tsuchida, and R. Sugizaki, "Multi-core fibers for large capacity SDM," OFC 2011, OWJ1 (2011).
34. J. Sakaguchi, Y. Awaji, N. Wada, T. Hayashi, T. Nagashima, T. Kobayashi, and M. Watanabe, "Propagation characteristics of seven-core fiber for spatial and wavelength division division multiplexed 10-Gbit/s channels," OFC 2011, OWJ2 (2011).
35. T. Hayashi, T. Nagashima, O. Shimakawa, T. Sasaki, and E. Sasaoka, "Crosstalk variation of multi-core fibre due to fibre bend," ECOC 2010, We.8.F.6 (2010).
36. J. M. Fini, B. Zhu, T. F. Taunay, and M. F. Yan, "Statistics of crosstalk in bent multicore fibers," Opt. Express **18**(14), 15122–15129 (2010).
37. M. Koshiba, K. Saitoh, K. Takenaga, and S. Matsuo, "Multi-core fiber design and analysis: coupled-mode theory and coupled-power theory," Opt. Express **19**(26), B102–B111 (2011).
38. S. Haykin, *Adaptive Filter Theory*, 4th ed. (Prentice Hall, 2002).
39. C. Xia, N. Bai, I. Ozdur, X. Zhou, and G. Li, "Supermodes for optical transmission," Opt. Express **19**(17), 16653–16664 (2011).

1. Introduction

The demand for high transmission capacity in fiber-optic communication systems has attracted considerable attention because of their various applications in long-haul links, data centers, and passive optical access networks (PONs) [1–3]. To overcome the capacity limit, technologies such as coherent detection [4], space division multiplexing using multi-core fibers (MCFs), and mode division multiplexing for multimode fibers (MMFs) based on Multiple-Input Multiple-Output (MIMO) signal processing have been proposed [5–11]. Among them, MCFs offer the advantages of device compactness, transceiver simplicity, and tolerance to intermodal dispersion in MMF systems [6, 12–15]. Numerous published works on MCFs have been focused on laser [16–19] and amplifier [20] applications but their use as a transmission medium in communication systems is relatively less investigated until recently. One of the design strategies for increasing the transmission capacity using MCFs is to realize high core density while minimizing cross-talks between signals in different cores so as to maintain transmission performance in each individual core [21]. To this end, a 7-core multi-

#156104 - $15.00 USD Received 10 Oct 2011; revised 20 Dec 2011; accepted 1 Feb 2012; published 9 Feb 2012

core fiber with transmission up to 112 Tb/s has been achieved [22]. Different core arrangement topologies have been investigated to maximize the core densities while minimizing cross-talks [5, 23, 24, 27]. The cross-talk analyses in most of the recent published works utilize a 2-core model, i.e. a directional coupler, as a guideline for cross-talk evaluation [21]. However, a detailed analysis on the coupling dynamics of the composite multi-core structure [25–27], transmission performance degradations due to mode coupling and appropriate communication strategies for MCF as a multiple-input-multiple-output (MIMO) system is yet to be undertaken.

In this paper, we analytically derive the overall mode coupling dynamics for 7-core MCFs for the case of identical cores and three types of cores. With mode coupling as cross-talks in a communication theory framework, we then study joint signal processing techniques for cross-talk mitigation and characterize corresponding transmission performance. For MCFs with homogeneous cores, we show that the coupling dynamics are aperiodic in general. This phenomenon was first reported in the 1980s in the context of coupled-mode theory [28] but has been overlooked in recent publications in MCF as MIMO systems in which a 2-core model is used for cross-talk analysis. A generalized definition of the coupling length is introduced as a descriptor to the aperiodic coupling dynamics of a composite waveguide such as a MCF. For heterogeneous MCFs with groups of cores that are identical within the group and dissimilar across different groups, it is shown that even though signals will not couple into neighboring dissimilar cores, the coupling dynamics within a group of identical cores are still very much affected by the presence of neighboring dissimilar cores. As a 7×7 MIMO system, we then proceed to investigate joint detection techniques for cross-talk mitigation such as the least mean square (LMS) algorithm and maximum-likelihood (ML) detection for coherent as well as intensity modulation formats. For intensity modulated systems, the aperiodic coupling dynamics prevent complete mitigation of cross-talks and lower bounds on the system bit-error-ratio (BER) are determined.

2. Coupled-mode formalism

We consider a MCF composed of n non-identical cores (labeled core 1, 2, …, n) arbitrarily embedded near the center of the cladding. The p^{th} core is identified by its radius and refractive index a_p and n_{1p} respectively while the cladding has a refractive index of n_2. The cores are spatially positioned such that the field from each core is relatively well isolated and perturbation methods with conventional coupled-mode theory can be used to analyze the mode coupling dynamics [29, 30]. We assume that each core only supports the LP_{01} fundamental mode and we denote the amplitude of the LP_{01} mode of the p^{th} core as $A_p(z)$. The simultaneous mode coupling between all the cores of a MCF is governed by a set of coupled-mode equations [29–31], which can be written in a matrix form as

$$\frac{\mathrm{d}\mathbf{A}(z)}{\mathrm{d}z} = -\mathbf{C}\mathbf{A}(z) \tag{1}$$

where $\mathbf{A}(z) = [A_1(z)\ A_2(z)\ \ldots\ A_n(z)]^{\mathrm{T}}$ is a column vector and T denotes the transpose, z is the direction of propagation, and $\mathbf{C}$ is a $n \times n$ matrix with elements c_{pq} given by

$$c_{pq} = \begin{cases} jC_{pq}\exp\left[j(\beta_p - \beta_q)z\right] & p \neq q, \\ 0 & p = q, \end{cases} \tag{2}$$

where β_p represents the propagation constant for the LP_{01} mode of core p. The coupling coefficient C_{pq} is a measure of the spatial overlapping of the mode fields of core p and q over the cross-sectional area of core q. Using the addition theorem [32] to express the mode field of core p in terms of the local coordinate system of core q and with the help of the eigenvalue equation for a step-index optical fiber, C_{pq} can be obtained analytically as

#156104 - $15.00 USD Received 10 Oct 2011; revised 20 Dec 2011; accepted 1 Feb 2012; published 9 Feb 2012

$$C_{pq} = \sqrt{2\Delta_q} W_q U_p K_0\left(\frac{W_p d_{pq}}{a_p}\right)\left[a_p U_q J_1(U_q) I_0\left(\frac{W_p a_q}{a_p}\right) + a_q W_p J_0(U_q) I_1\left(\frac{W_p a_q}{a_p}\right)\right]\left[V_p J_1(U_q) K_1(W_p)\left(a_p^2 U_q^2 + a_q^2 W_p^2\right)\right]^{-1} \tag{3}$$

where J_l, I_l, and K_l are the Bessel function of the first kind and the modified Bessel functions of the first and second kinds of order l respectively and d_{pq} is the distance between the centers of core p and q. The normalized fiber parameters U_p, V_p, and W_p are defined as $U_p = a_p [(2\pi n_{1p}/\lambda)^2 - \beta_p^2]^{1/2}$, $V_p = a_p (2\pi/\lambda)(n_{1p}^2 - n_2^2)^{1/2}$, and $W_p = a_p [\beta_p^2 - (2\pi n_2/\lambda)^2]^{1/2}$ with λ being the free-space wavelength. The index contrast $\Delta_p = (n_{1p}^2 - n_2^2)/(2n_{1p}^2)$ can be approximated as $(n_{1p} - n_2)/n_{1p}$ which corresponds to the relative core-cladding index difference. The electric field of the individual core, denoted as $E_p(z)$, can be expressed in terms of its mode amplitude $A_p(z)$ as

$$E_p(z) = A_p(z) \exp(-j\beta_p z). \tag{4}$$

Equation (1) cannot be solved readily because the elements in **C** are z-dependent. Using Eq. (4), we can translate Eq. (1) to an eigenvalue problem

$$\frac{d\mathbf{E}(z)}{dz} = -\mathbf{R}\mathbf{E}(z) \tag{5}$$

where $\mathbf{E}(z) = [E_1(z)\ E_2(z)\ \ldots\ E_n(z)]^T$ and **R** contains z-independent elements r_{pq} given by

$$r_{pq} = \begin{cases} jC_{pq} & p \neq q, \\ j\beta_p & p = q. \end{cases} \tag{6}$$

Using the substitution $\mathbf{E}(z) = \exp(-\mathbf{R}z)\mathbf{E}(0)$, the solution to Eq. (5) is obtained as

$$\mathbf{E}(z) = \mathbf{V}\left[\exp(-\gamma_p z)\delta_{pq}\right]\mathbf{V}^{-1}\mathbf{E}(0) \tag{7}$$

and

$$\mathbf{V} = \left[\mathbf{v}_1\ \mathbf{v}_2 \ldots \mathbf{v}_n\right] \tag{8}$$

where δ_{pq} is the Kronecker delta function, γ_p is an eigenvalue of **R**, and $\mathbf{v}_p$ is the corresponding eigenvector. Equation (7) is a generalized solution for an n-core MCF that describes the power exchange between the modes of individual cores as the light propagates.

In the following sections, we analytically study the propagation dynamics of 7-core MCFs consisting of a center core (namely, core 1) surrounded by six cores (namely, core 2, 3, …, 7) arranged in a triangular lattice and illustrate the theoretical results with numerical examples. Unless otherwise specified, we assume that the pitch Λ = 30 μm, which is so chosen to maintain equal distance between the core and ambient for all the cores with a typical cladding radius of 62.5 μm. We assume the cladding index n_2 = 1.4440 (pure silica at 1.550 μm) and identical core radii a_p = 4.5 μm for all p = 1, 2, …, 7. Of course, the analytical derivations can be well applied to other 7-core MCFs reported in recent experiments with various geometry and index profiles [33, 34].

3. Analysis of mode coupling dynamics in multi-core fibers

3.1 Homogeneous 7-core MCF

We first study the simplest case with $\Delta_p = \Delta$ for all p, i.e. a homogeneous 7-core MCF as shown in Fig. 1. The coupled-mode equations are given by Eq. (1) with the matrix

#156104 - $15.00 USD Received 10 Oct 2011; revised 20 Dec 2011; accepted 1 Feb 2012; published 9 Feb 2012

$$\mathbf{C} = j\begin{bmatrix} 0 & C_{12} & C_{12} & C_{12} & C_{12} & C_{12} & C_{12} \\ C_{12} & 0 & C_{12} & 0 & 0 & 0 & C_{12} \\ C_{12} & C_{12} & 0 & C_{12} & 0 & 0 & 0 \\ C_{12} & 0 & C_{12} & 0 & C_{12} & 0 & 0 \\ C_{12} & 0 & 0 & C_{12} & 0 & C_{12} & 0 \\ C_{12} & 0 & 0 & 0 & C_{12} & 0 & C_{12} \\ C_{12} & C_{12} & 0 & 0 & 0 & C_{12} & 0 \end{bmatrix} \tag{9}$$

where the off-diagonal zeros correspond to pairs of cores assumed to have negligible coupling due to large inter-core distances. Translating **C** into **R** using Eq. (6) yields a sequence of eigenvalues in increasing mode order given by

$$\gamma_1 = jC_{12}(1+\sqrt{7}),\ \gamma_2 = \gamma_3 = jC_{12},\ \gamma_4 = \gamma_5 = -jC_{12},\ \gamma_6 = jC_{12}(1-\sqrt{7}),\ \gamma_7 = -2jC_{12} \tag{10}$$

and C_{pq} is given by Eq. (3). When light is launched into core 1, i.e. $A_1(0) = 1$ and $A_p(0) = 0$ for $p \neq 1$, analytical solutions for the mode amplitudes at distance z are obtained as

$$A_1(z) = \left[\cos\left(\sqrt{7}C_{12}z\right) + \frac{j}{\sqrt{7}}\sin\left(\sqrt{7}C_{12}z\right)\right]\exp\left(-jC_{12}z\right) \tag{11}$$

and

$$A_p(z) = -\frac{j}{\sqrt{7}}\sin\left(\sqrt{7}C_{12}z\right)\exp\left(-jC_{12}z\right) \qquad p \neq 1 \tag{12}$$

while the normalized mode powers $|A_p(z)|^2$ can be expressed as

$$\left|A_1(z)\right|^2 = \frac{1}{7} + \frac{6}{7}\cos^2\left(\sqrt{7}C_{12}z\right) \tag{13}$$

and

$$\left|A_p(z)\right|^2 = \frac{1}{7}\sin^2\left(\sqrt{7}C_{12}z\right) \qquad p \neq 1, \tag{14}$$

which are periodic in z. The minima of $|A_1(z)|^2$ are located at the maxima of $|A_p(z)|^2$. According to Eq. (13), the normalized mode power drops to its first minimum at a distance $\mathcal{L}_{c1}$ given by

$$\mathcal{L}_{c1} = \frac{\pi}{2\sqrt{7}C_{12}} = \frac{\pi}{\left|-j(\gamma_1 - \gamma_6)\right|}, \tag{15}$$

which is shorter than that of a 2-core model by a factor of $\sqrt{7}$. The signal power of the launching core at $z = \mathcal{L}_{c1}$ is equal to

$$\left|A_1(\mathcal{L}_{c1})\right|^2 = \frac{1}{7}. \tag{16}$$

#156104 - $15.00 USD Received 10 Oct 2011; revised 20 Dec 2011; accepted 1 Feb 2012; published 9 Feb 2012

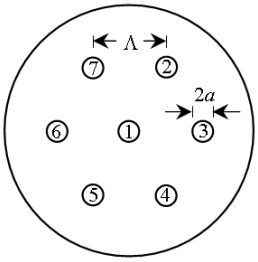

Fig. 1. Homogeneous 7-core MCF arranged in a triangular lattice with pitch Λ and core radius *a*.

When light is launched into core 2, i.e. $A_2(0) = 1$ and $A_p(0) = 0$ for $p \neq 2$, the mode amplitudes for various cores are given by

$$A_1(z) = -\frac{j}{\sqrt{7}}\sin\left(\sqrt{7}C_{12}z\right)\exp\left(-jC_{12}z\right), \tag{17}$$

$$A_2(z) = \frac{2}{3}\cos\left(C_{12}z\right) + \frac{1}{6}\exp\left(2jC_{12}z\right) + \frac{1}{6}\exp\left(-jC_{12}z\right)\left[\cos\left(\sqrt{7}C_{12}z\right) - \frac{j}{\sqrt{7}}\sin\left(\sqrt{7}C_{12}z\right)\right], \tag{18}$$

$$A_3(z) = A_7(z) = -\frac{j}{3}\sin\left(C_{12}z\right) - \frac{1}{6}\exp\left(2jC_{12}z\right) + \frac{1}{6}\exp\left(-jC_{12}z\right)\left[\cos\left(\sqrt{7}C_{12}z\right) - \frac{j}{\sqrt{7}}\sin\left(\sqrt{7}C_{12}z\right)\right], \tag{19}$$

$$A_4(z) = A_6(z) = -\frac{1}{3}\cos\left(C_{12}z\right) + \frac{1}{6}\exp\left(2jC_{12}z\right) + \frac{1}{6}\exp\left(-jC_{12}z\right)\left[\cos\left(\sqrt{7}C_{12}z\right) - \frac{j}{\sqrt{7}}\sin\left(\sqrt{7}C_{12}z\right)\right], \tag{20}$$

and

$$A_5(z) = j\frac{2}{3}\sin\left(C_{12}z\right) - \frac{1}{6}\exp\left(2jC_{12}z\right) + \frac{1}{6}\exp\left(-jC_{12}z\right)\left[\cos\left(\sqrt{7}C_{12}z\right) - \frac{j}{\sqrt{7}}\sin\left(\sqrt{7}C_{12}z\right)\right]. \tag{21}$$

Some of the mode amplitudes are identical due to symmetry. The propagation dynamics of a 7-core MCF when light is launched into core 2 are shown in Fig. 2. In addition to unequal coupling to different cores, launching into core 2 (or other outer cores) also leads to aperiodic coupling for all the cores except the center core. Although aperiodic coupling has been reported in [28] in the context of coupled-mode theory, most of the recent reported analyses on mode coupling in MCFs as transmission fibers utilize a 2-core model [21] or focus on cases in which light is launched into the center core [29, 35–37]. From a communication theory perspective, aperiodic mode coupling will result in cross-talks in the MIMO MCF system that is aperiodic over transmission distance. To describe the aperiodic coupling dynamics and aid our subsequent discussion on joint signal processing techniques for MCF systems, we introduce a generalized coupling length $\mathcal{L}_{cp}$, defined as the propagation length at which the normalized mode power in the p^{th} launching core drops from one to its first minimum. This definition is general as it incorporates both aperiodic and periodic coupling dynamics. The generalized coupling length $\mathcal{L}_{c2}$ can be calculated numerically from Eq. (18) by setting its first derivative $\mathrm{d}A_2(z)/\mathrm{d}z|_{z=\mathcal{L}_{c2}} = 0$ which is given by

$$\mathcal{L}_{c2} = 1.585/C_{12} \tag{22}$$

#156104 - $15.00 USD Received 10 Oct 2011; revised 20 Dec 2011; accepted 1 Feb 2012; published 9 Feb 2012

with corresponding mode power

$$|A_2(\mathcal{L}_{c2})|^2 = 2.040\times10^{-2} \tag{23}$$

which is independent of fiber geometry and index contrasts. Locations of the first maxima and their corresponding mode powers are $\pi/(2\sqrt{7}\,C_{12})$ and 1/7, $0.6622/C_{12}$ and 0.1681, $1.024/C_{12}$ and 0.1927, and $1.550/C_{12}$ and 0.6187 for core 1, 3, 4, and 5, respectively. The generalized coupling length serves as a measure for evaluating the coupling strength of composite waveguides such as MCFs. The dependency of the generalized coupling lengths $\mathcal{L}_{c1}$ and $\mathcal{L}_{c2}$ on the relative index difference Δ is shown in Fig. 3 for different pitch values Λ. The normalized mode powers at $\mathcal{L}_{c1}$ and $\mathcal{L}_{c2}$ are obtained from Eqs. (16) and (23), respectively. As shown in Fig. 3, $\mathcal{L}_{c1}$ is smaller than $\mathcal{L}_{c2}$ and both of them increase with Δ or Λ.

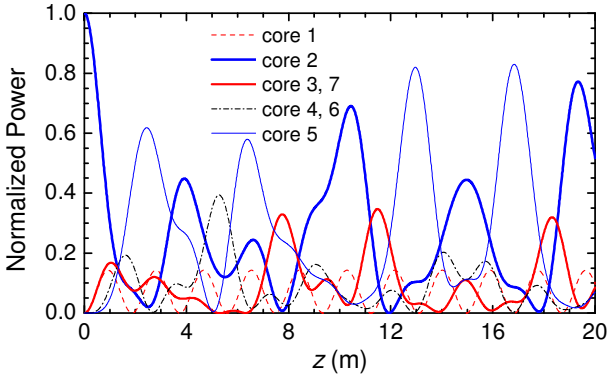

Fig. 2. Propagation dynamics of a homogeneous 7-core MCF with Λ = 30 μm, a = 4.5 μm, and Δ = 0.370% for the case of light launching into core 2. The aperiodic coupling dynamics cannot be predicted by a 2-core model, thus indicating its inadequacy for the analysis of mode coupling and cross-talks in MCFs as MIMO transmission systems.

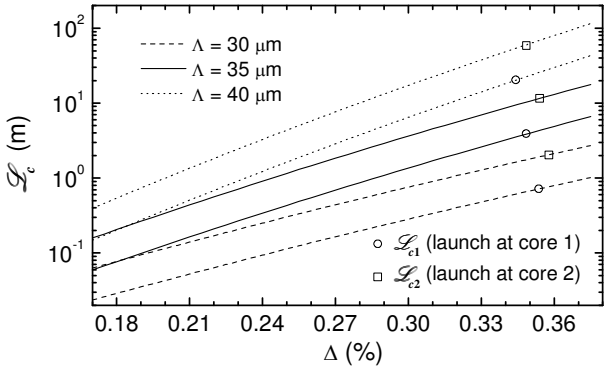

Fig. 3. Generalized coupling lengths $\mathcal{L}_c$ of a homogeneous 7-core MCF as a function of the relative index difference Δ for pitch values of 30, 35, and 40 μm. The core radius is 4.5 μm.

3.2 Heterogeneous 7-core MCF with three types of cores

In this section, we consider a MCF with $\Delta_2 = \Delta_4 = \Delta_6$, $\Delta_3 = \Delta_5 = \Delta_7$, and $\Delta_1 \neq \Delta_2 \neq \Delta_3$ as shown in Fig. 4, which is a configuration that has attracted most of the attention to date [5, 14].

The 7-core MCF is composed of a center core plus two core groups with each group having three identical cores. The matrix **C** is given by

#156104 - $15.00 USD Received 10 Oct 2011; revised 20 Dec 2011; accepted 1 Feb 2012; published 9 Feb 2012

$$\mathbf{C} = j \times \begin{bmatrix} 0 & C_{12}e^{j\Delta\beta_{12}z} & C_{13}e^{j\Delta\beta_{13}z} & C_{12}e^{j\Delta\beta_{12}z} & C_{13}e^{j\Delta\beta_{13}z} & C_{12}e^{j\Delta\beta_{12}z} & C_{13}e^{j\Delta\beta_{13}z} \\ C_{21}e^{j\Delta\beta_{21}z} & 0 & C_{23}e^{j\Delta\beta_{23}z} & C_{24} & 0 & C_{24} & C_{23}e^{j\Delta\beta_{23}z} \\ C_{31}e^{j\Delta\beta_{31}z} & C_{32}e^{j\Delta\beta_{32}z} & 0 & C_{32}e^{j\Delta\beta_{32}z} & C_{35} & 0 & C_{35} \\ C_{21}e^{j\Delta\beta_{21}z} & C_{24} & C_{23}e^{j\Delta\beta_{23}z} & 0 & C_{23}e^{j\Delta\beta_{23}z} & C_{24} & 0 \\ C_{31}e^{j\Delta\beta_{31}z} & 0 & C_{35} & C_{32}e^{j\Delta\beta_{32}z} & 0 & C_{32}e^{j\Delta\beta_{32}z} & C_{35} \\ C_{21}e^{j\Delta\beta_{21}z} & C_{24} & 0 & C_{24} & C_{23}e^{j\Delta\beta_{23}z} & 0 & C_{23}e^{j\Delta\beta_{23}z} \\ C_{31}e^{j\Delta\beta_{31}z} & C_{32}e^{j\Delta\beta_{32}z} & C_{35} & 0 & C_{35} & C_{32}e^{j\Delta\beta_{32}z} & 0 \end{bmatrix} \tag{24}$$

where $\Delta\beta_{pq} = \beta_p - \beta_q$. The eigenvalues can be calculated explicitly as

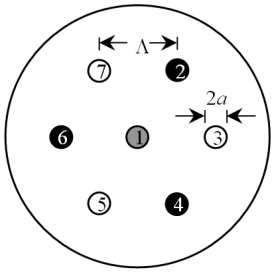

Fig. 4. Heterogeneous 7-core MCF with three types of cores: $\Delta_2 = \Delta_4 = \Delta_6$, $\Delta_3 = \Delta_5 = \Delta_7$, and $\Delta_1 \neq \Delta_2 \neq \Delta_3$.

$$\gamma_1 = \gamma_6 = j\left[\bar{\alpha}_2 + \bar{\alpha}_3 + \sqrt{(\bar{\alpha}_2 - \bar{\alpha}_3)^2 + C_{23}C_{32}} + \beta_1\right], \quad \gamma_2 = \gamma_7 = j\left[\bar{\alpha}_2 + \bar{\alpha}_3 - \sqrt{(\bar{\alpha}_2 - \bar{\alpha}_3)^2 + C_{23}C_{32}} + \beta_1\right],$$
$$\gamma_3 = j\left(g + h + \frac{\alpha_2 + \alpha_3}{3} + \beta_1\right), \quad \gamma_4 = \frac{\sqrt{3}}{2}(g - h) + j\left[-\frac{1}{2}(g + h) + \frac{\alpha_2 + \alpha_3}{3} + \beta_1\right],$$
$$\gamma_5 = -\frac{\sqrt{3}}{2}(g - h) + j\left[-\frac{1}{2}(g + h) + \frac{\alpha_2 + \alpha_3}{3} + \beta_1\right] \tag{25}$$

where

$$\alpha_2 = \beta_2 - \beta_1 + 2C_{24}, \quad \alpha_3 = \beta_3 - \beta_1 + 2C_{35}, \tag{26}$$

$$\bar{\alpha}_2 = \frac{\beta_2 - \beta_1 - C_{24}}{2}, \quad \bar{\alpha}_3 = \frac{\beta_3 - \beta_1 - C_{35}}{2}, \tag{27}$$

$$u = \alpha_2\alpha_3 - 3(C_{12}C_{21} + C_{13}C_{31}) - 4C_{23}C_{32} - \frac{1}{3}(\alpha_2 + \alpha_3)^2, \tag{28}$$

$$v = -\frac{2}{27}(\alpha_2 + \alpha_3)^3 + \frac{1}{3}(\alpha_2 + \alpha_3)\left[\alpha_2\alpha_3 - 3(C_{12}C_{21} + C_{13}C_{31}) - 4C_{23}C_{32}\right] + 3(C_{13}C_{31}\alpha_2 + C_{12}C_{21}\alpha_3) - 6(C_{32}C_{13}C_{21} + C_{12}C_{23}C_{31}), \tag{29}$$

$$g = \left\{-\frac{v}{2} + \left[\left(\frac{u}{3}\right)^3 + \left(\frac{v}{2}\right)^2\right]^{1/2}\right\}^{1/3}, \quad h = \left\{-\frac{v}{2} - \left[\left(\frac{u}{3}\right)^3 + \left(\frac{v}{2}\right)^2\right]^{1/2}\right\}^{1/3}. \tag{30}$$

#156104 - $15.00 USD Received 10 Oct 2011; revised 20 Dec 2011; accepted 1 Feb 2012; published 9 Feb 2012

In this case, analytical solutions to the mode amplitudes for various cores are difficult to obtain. However, if the cores are well-isolated such that no power is coupled into dissimilar cores (which is the original objective of designing heterogeneous MCFs anyway), we can treat the 7-core MCF as two groups of 3-core MCFs and a single core at the center with no power transfer between these groups. Nonetheless, for this type of composite waveguides in which there is no coupling between groups of dissimilar cores, the Appendix illustrates how the generalized coupling lengths for an individual group of identical cores are dependent on the eigenvalues in Eq. (25) and are significantly affected by the presence of neighboring dissimilar cores. Consequently, to characterize the coupling dynamics for the heterogeneous 7-core MCF when light is launched into cores 2, 3, 4, 5, 6, or 7, we first study the corresponding homogeneous 3-core MCF in which the coupling within the homogeneous cores are known to be periodic. Afterwards, the generalized coupling lengths of the composite 7-core structure are semi-analytically determined from different combinations of eigenvalues in Eq. (25). For light launching into core 2, the mode powers are found to be

$$\begin{cases} \left|A_2(z)\right|^2=\frac{1}{9}+\frac{8}{9}\cos^2\left[\frac{-j(\gamma_2-\gamma_5)z}{2}\right], \quad \left|A_4(z)\right|^2=\left|A_6(z)\right|^2=\frac{4}{9}\sin^2\left[\frac{-j(\gamma_2-\gamma_5)z}{2}\right] & \text{for } \Delta_2<\Delta_1,\Delta_3 \\ \left|A_2(z)\right|^2=\frac{1}{9}+\frac{8}{9}\cos^2\left[\frac{-j(\gamma_1-\gamma_3)z}{2}\right], \quad \left|A_4(z)\right|^2=\left|A_6(z)\right|^2=\frac{4}{9}\sin^2\left[\frac{-j(\gamma_1-\gamma_3)z}{2}\right] & \text{for } \Delta_2>\Delta_1,\Delta_3 \\ \left|A_2(z)\right|^2=\frac{1}{9}+\frac{8}{9}\cos^2\left[\frac{-j(\gamma_2-\gamma_4)z}{2}\right], \quad \left|A_4(z)\right|^2=\left|A_6(z)\right|^2=\frac{4}{9}\sin^2\left[\frac{-j(\gamma_2-\gamma_4)z}{2}\right] & \text{for } \Delta_1<\Delta_2<\Delta_3 \\ \left|A_2(z)\right|^2=\frac{1}{9}+\frac{8}{9}\cos^2\left[\frac{-j(\gamma_1-\gamma_4)z}{2}\right], \quad \left|A_4(z)\right|^2=\left|A_6(z)\right|^2=\frac{4}{9}\sin^2\left[\frac{-j(\gamma_1-\gamma_4)z}{2}\right] & \text{for } \Delta_3<\Delta_2<\Delta_1 \end{cases} \tag{31}$$

from which we obtain

$$\boldsymbol{\mathcal{L}}_{c2}=\begin{cases} \pi/\left|-j(\gamma_2-\gamma_5)\right| & \text{for } \Delta_2<\Delta_1,\Delta_3 \\ \pi/\left|-j(\gamma_1-\gamma_3)\right| & \text{for } \Delta_2>\Delta_1,\Delta_3 \\ \pi/\left|-j(\gamma_2-\gamma_4)\right| & \text{for } \Delta_1<\Delta_2<\Delta_3 \\ \pi/\left|-j(\gamma_1-\gamma_4)\right| & \text{for } \Delta_3<\Delta_2<\Delta_1 \end{cases} \tag{32}$$

and

$$|A_2(\boldsymbol{\mathcal{L}}_{c2})|^2=1/9. \tag{33}$$

#156104 - $15.00 USD Received 10 Oct 2011; revised 20 Dec 2011; accepted 1 Feb 2012; published 9 Feb 2012

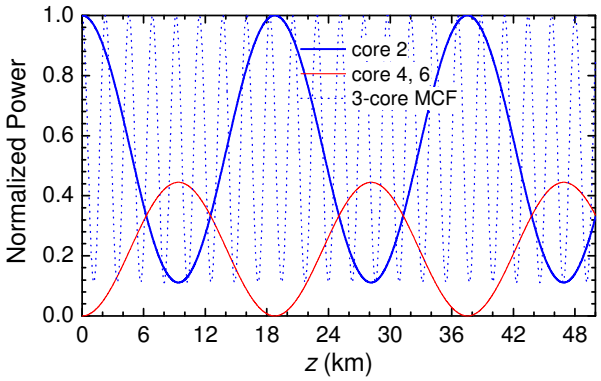

Fig. 5. Propagation dynamics for a 7-core MCF with $\Delta_1 = 0.370\%$, $\Delta_2 = \Delta_4 = \Delta_6 = 0.325\%$, $\Delta_3 = \Delta_5 = \Delta_7 = 0.360\%$, $\Lambda = 30$ μm, and $a = 4.5$ μm when light is launched into core 2. The coupling dynamics for a corresponding homogeneous 3-core MCF in the absence of core 1, 3, 5, and 7 is also shown. The coupling features of the 7-core MCF resemble those of a homogeneous 3-core MCF but the generalized coupling length are very different.

When light is launched into core 3, the mode solutions, generalized coupling length $\mathcal{L}_{c3}$, and the modal power $|A_3(\mathcal{L}_{c3})|^2$ can be obtained from Eqs. (31), (32), and (33) respectively by switching Δ_2 with Δ_3, $A_2(z)$ with $A_3(z)$, $A_4(z)$ with $A_5(z)$, $A_6(z)$ with $A_7(z)$, and $\mathcal{L}_{c2}$ with $\mathcal{L}_{c3}$. Light launching into core 1 simply does not couple out i.e. $|A_1(z)|^2 = 1$ and $|A_p(z)|^2 = 0$ for $p \neq 1$. The propagation dynamics of a heterogeneous 7-core MCF with $\Delta_1 = 0.370\%$, $\Delta_2 = \Delta_4 = \Delta_6 = 0.325\%$, and $\Delta_3 = \Delta_5 = \Delta_7 = 0.360\%$ are shown in Fig. 5 for the case when light is launched into core 2 along with that of a homogeneous 3-core MCF (assuming cores 1, 3, 5, and 7 are absent) for comparison. The generalized coupling lengths for the two cases are 9.38 and 1.14 km respectively, indicating the strong effect of cores 1, 3, 5, and 7 on coupling dynamics of core 2, 4, and 6.

The dependence of $\mathcal{L}_{c2}$ and $\mathcal{L}_{c3}$ on Δ_2 is shown in Fig. 6 for various combinations of Δ_1 and Δ_3. From the figure, the generalized coupling lengths can increase substantially as the eigenvalues in Eq. (32) become close to each other, which can be identified from the peaks in Fig. 6. This can be understood as the case when the propagation constants of different eigenmodes of the composite MCF structure become equal. On the other hand, the dips in Fig. 6 correspond to cases where $\Delta_1 = \Delta_2$, $\Delta_1 = \Delta_3$, and/or $\Delta_2 = \Delta_3$ for which the generalized coupling lengths drop because of enhanced coupling between core groups.

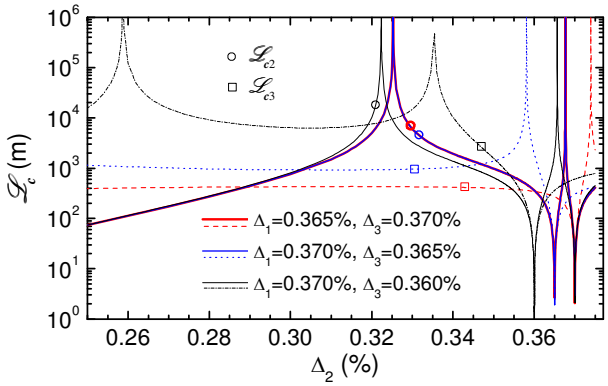

Fig. 6. Dependence of $\mathcal{L}_{c2}$ and $\mathcal{L}_{c3}$ on Δ_2 for various combinations of Δ_1 and Δ_3. The generalized coupling lengths decrease when the cores become similar and increase when the eigenvalues of the coupling matrix $\mathbf{R}$ (or propagation constants of the eigenmodes of the composite MCF) given in Eq. (5) become similar.

#156104 - $15.00 USD Received 10 Oct 2011; revised 20 Dec 2011; accepted 1 Feb 2012; published 9 Feb 2012

4. Communication strategies and transmission performance for 7-core MCFs in the presence of mode coupling

One of the major objectives for studying mode coupling dynamics in MCFs is to characterize cross-talks between cores and potentially derive appropriate joint signal processing techniques to mitigate the cross-talks and/or optimally detect the transmitted signals. We will hereby investigate communication strategies for a homogenous 7-core MCF as its coupling dynamics are more complex than that of heterogeneous-core MCFs. Neglecting polarization effects and inter-symbol interference (ISI) induced by chromatic dispersion, one can model the 7-core MCF as a memory-less 7 × 7 multiple-input-multiple-output (MIMO) system. In this case, for a given input signal

$$\mathbf{E}(0) = \left[E_1(0)\ \ E_2(0)\ \ E_3(0)\ \ E_4(0)\ \ E_5(0)\ \ E_6(0)\ \ E_7(0)\right]^{\mathrm{H}}, \tag{34}$$

the output at the receiving end of the MCF with length z is given by

$$\mathbf{E}(z) = e^{-\mathbf{R}z}\mathbf{E}(0) = \mathbf{T}\mathbf{E}(0). \tag{35}$$

For systems with coherent detection, the balanced detector outputs $\mathbf{y} = [y_1\ y_2\ y_3\ y_4\ y_5\ y_6\ y_7]^{\mathrm{T}}$ can be expressed as

$$y_p = E_p(z) + \upsilon_p, \qquad p = 1,2,3,4,5,6,7 \tag{36}$$

where $\boldsymbol{\upsilon} = [\upsilon_1\ \upsilon_2\ \upsilon_3\ \upsilon_4\ \upsilon_5\ \upsilon_6\ \upsilon_7]^{\mathrm{T}}$ are independent identically distributed (i.i.d) additive white Gaussian noise (AWGN) that collectively model shot noise and thermal noise from the photo receivers. In principle, one can equalize the channel and obtain a joint estimate of the transmitted signal $\hat{\mathbf{E}}(0)$ simply by

$$\hat{\mathbf{E}}(0) = \mathbf{T}^{-1}\mathbf{y} = \mathbf{W}^H\mathbf{y} = \mathbf{E}(0) + \mathbf{W}^H\boldsymbol{\upsilon}. \tag{37}$$

Since $\mathbf{T}$ is unitary, $\mathbf{W}^H\boldsymbol{\upsilon}$ are i.i.d. AWGN with the same covariance matrix as $\boldsymbol{\upsilon}$ and hence the effects of cross-talks or mode coupling can be perfectly compensated. In practice however, the coupling dynamics will be distorted by bending and other fabrication imperfections such that $\mathbf{W}^H$ may not be known. In this case, adaptive signal processing techniques such as the least mean squares (LMS) algorithm will most likely be used to 'learn' the channel and mitigate cross-talks. In particular, N sets of training data $\mathbf{E}^{(1)}(0), \mathbf{E}^{(2)}(0), \cdots \mathbf{E}^{(N)}(0)$ are transmitted and the $n + 1^{\text{th}}$ update of $\mathbf{W}$ is given by [38]

$$\mathbf{W}^{(n+1)} = \mathbf{W}^{(n)} + \mu\mathbf{y}^{(n)}\left(\mathbf{E}^{(n)}(0) - \left(\mathbf{W}^{(n)}\right)^H \mathbf{y}^{(n)}\right)^H = \mathbf{W}^{(n)} + \mu\mathbf{y}^{(n)}e(n)^H \tag{38}$$

where μ is the step size of the LMS update, $\mathbf{y}^{(n)}$ is the n^{th} received vector and $e(n)$ is the error vector. For a signal-to-noise ratio (SNR) of 20 dB, the convergence behavior of the LMS algorithm for a homogeneous 7-core fiber using quadrature phase-shift-keying (QPSK) modulation format are shown in Fig. 7 with different step sizes. The propagation distance is $z = \mathcal{L}_c$ and the initial state is set to be $\mathbf{W}^{(1)} = \mathbf{I}$. It can be seen that when the step size is large enough, convergence can be achieved with around 100 to 200 symbols. Further simulation results suggest that the speed of convergence stays more or less the same for $z > 0.5\ \mathcal{L}_c$.

#156104 - $15.00 USD Received 10 Oct 2011; revised 20 Dec 2011; accepted 1 Feb 2012; published 9 Feb 2012

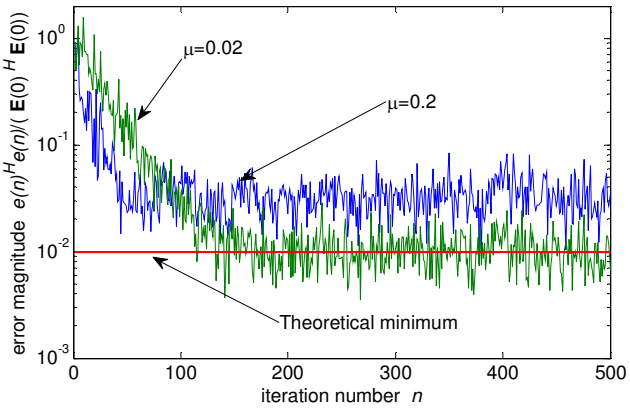

Fig. 7. Convergence behavior using the LMS algorithm for equalizing mode coupling induced cross-talks for a homogenous 7-core fiber system with QPSK signals. The SNR is 20 dB and the propagation distance is $z = \mathcal{L}_c$.

On the other hand, for on-off keying (OOK) systems with direct detection in which information is encoded in the amplitude of $\mathbf{E}(0)$ i.e. $\mathbf{E}(0) \in \{0, 1\}^7$, the output signal is given by

$$\begin{aligned} s_p &= \left|E_p(z)\right|^2 + \upsilon_p \\ &= \left|\mathbf{t}_p \mathbf{E}(0)\right|^2 + \upsilon_p \end{aligned} \tag{39}$$

where $\mathbf{t}_p$ is the p^{th} row of $\mathbf{T}$. Unfortunately, due to the magnitude squared operation by the photo-diode, linear equalization techniques cannot fully equalize or eliminate the cross-talks. Figure 8 shows the convergence behavior of the LMS algorithm for an OOK system with transmission distance $z = \mathcal{L}_c$. The SNR is 20dB and the initial state of the equalization filter is set to be $\mathbf{W}^{(1)} = \mathbf{I}$. It is obvious from the convergence behavior that only a small amount of cross-talk can be mitigated by the LMS algorithm and subsequent transmission performance using linear equalization is far from that of a cross-talk-free system. Further simulation results with larger number of LMS iterations and smaller step sizes do not help reduce the cross-talks.

To understand such performance limitations in further detail, one can jointly model the transmitted OOK signals in the 7-core MCF as a set of 128 signal points in a 7-dimensional signal space. The locations of the constellation points depend on z and $\mathbf{T}$ and such constellations are irregular in general. In this case, joint Maximum-likelihood detection on the received signals $\mathbf{y}$ can be described as

$$\hat{\mathbf{E}}(0) = \arg\min_{\mathbf{x} \in \{0,1\}^7} \left(\mathbf{s} - \left|\mathbf{T}\mathbf{x}\right|^2 \right)^{\mathrm{T}} \left(\mathbf{s} - \left|\mathbf{T}\mathbf{x}\right|^2 \right). \tag{40}$$

#156104 - $15.00 USD Received 10 Oct 2011; revised 20 Dec 2011; accepted 1 Feb 2012; published 9 Feb 2012

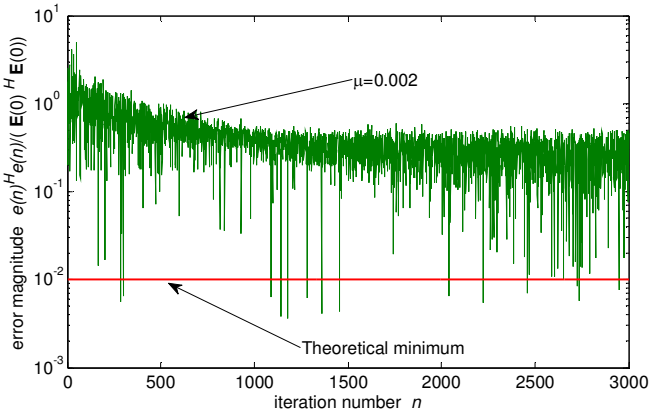

Fig. 8. Convergence behavior using the LMS algorithm for equalizing mode coupling induced cross-talks for a homogenous 7-core fiber system with OOK signals and direct detection. The SNR is 20 dB and the propagation distance is $z = \mathcal{L}_c$.

A lower bound of the system BER can be obtained by assuming that detection errors are mostly contributed by two particular signal constellation points in the 7-dimensional constellation that are closest to each other. Note that such lower bound is tight for high SNR. A plot of the BER lower bound for a homogeneous 7-core MCF is shown in Fig. 9 as a function of transmission distance z. From the figure, it can be seen that the BER lower bounds are aperiodic with z due to the aperiodic coupling dynamics of homogeneous 7-core MCF described in Section 3A. Starting from $z = 0$, the transmission performance degrades with z and approximately stays constant for $z > \mathcal{L}_{c1}$ and the performance does not approach back to that at $z = 0$. As ML detection is already the optimal receiver-based detection techniques, further performance improvements may be obtained from pre-coding at the transmitters such as signal constellation optimizations and/or new coding strategies for MCF systems.

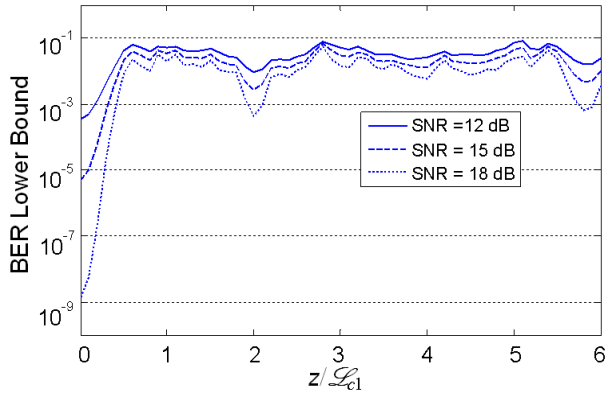

Fig. 9. BER lower bound for a homogeneous 7-core MCF with OOK modulation format and joint ML detection as a function of transmission distance. As the mode coupling dynamics is aperiodic, the lower bound is also aperiodic with z and transmission performance does not approach back to that at $z = 0$.

5. Conclusions

In this paper, we presented a detailed theoretical analysis of mode coupling dynamics for 7-core MCFs with identical cores and three types of cores. The coupling dynamics in a 7-core MCF with identical cores can be aperiodic along the propagation direction in general. A generalized definition of the coupling length is introduced to describe aperiodic coupling

#156104 - $15.00 USD Received 10 Oct 2011; revised 20 Dec 2011; accepted 1 Feb 2012; published 9 Feb 2012

dynamics in such composite waveguide structure. For heterogeneous 7-core MCFs designed to confine signal power transfer within a group of identical cores, the coupling dynamics in each group are considerably affected by the presence of neighboring dissimilar cores. Joint signal processing and detection strategies and corresponding transmission performance are also investigated for coherent as well as intensity modulated formats. The analytical insights obtained provide a more complete understanding of signal transmission and cross-talks in MCFs, which will help facilitate future MCF designs with appropriate signal processing techniques to realize high speed transmissions using spatially compact multi-core fibers. Extensions of the analysis to MCFs with arbitrarily number of cores and the effects of bending on mode coupling will be investigated in future works.

Appendix

Effect of neighboring dissimilar cores on coupling dynamics of a group of identical cores

Here we attempt to use the simplest model to analyze the coupling dynamics of MCFs consisting of different groups of identical cores and illustrate how it is affected by neighboring dissimilar cores. The simplest structure is a 4-core MCF having two types of cores as shown in Fig. 10 with $\Delta_2 = \Delta_4$ and $\Delta_3 = \Delta_5$. The eigenvalues of this 4-core MCF are analytically given by

$$\gamma_1 = j\left(\beta_2 - C_{24}\right),\ \ \gamma_2 = j\left(\beta_3 - C_{35}\right),\ \ \gamma_3 = j\left(\alpha_{22} + \alpha_{33} + \bar{S}\right),\ \ \gamma_4 = j\left(\alpha_{22} + \alpha_{33} - \bar{S}\right) \quad (41)$$

where

$$\alpha_{22} = \frac{\beta_2 + C_{24}}{2},\ \ \alpha_{33} = \frac{\beta_3 + C_{35}}{2},\ \ \bar{S} = \sqrt{\left(\alpha_{22} - \alpha_{33}\right)^2 + 4C_{23}C_{32}} \quad (42)$$

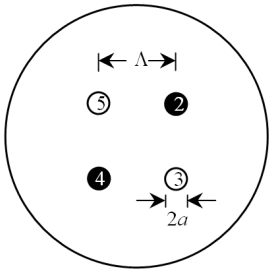

Fig. 10. Schematic diagram of a heterogeneous 4-core MCF consisting of two groups of identical cores: $\Delta_2 = \Delta_4$ and $\Delta_3 = \Delta_5$.

When light is launched into core 2, the solutions for the mode amplitudes are given by

$$A_2(z) = \frac{1}{2}\exp\left[-j\left(\alpha_{22} + \alpha_{33} - \beta_2\right) z\right]\left[\cos\left(\bar{S}z\right) - j\frac{\alpha_{22} - \alpha_{33}}{\bar{S}}\sin\left(\bar{S}z\right)\right] + \frac{1}{2}\exp\left(jC_{24}z\right), \quad (43)$$

$$A_4(z) = \frac{1}{2}\exp\left[-j\left(\alpha_{22} + \alpha_{33} - \beta_2\right) z\right]\left[\cos\left(\bar{S}z\right) - j\frac{\alpha_{22} - \alpha_{33}}{\bar{S}}\sin\left(\bar{S}z\right)\right] - \frac{1}{2}\exp\left(jC_{24}z\right), \quad (44)$$

and

$$A_3(z) = A_5(z) = -j\frac{C_{32}}{\bar{S}}\exp\left[-j\left(\alpha_{22} + \alpha_{33} - \beta_3\right) z\right]\ \sin\left(\bar{S}z\right), \quad (45)$$

from which the normalized mode powers can be calculated as

#156104 - $15.00 USD Received 10 Oct 2011; revised 20 Dec 2011; accepted 1 Feb 2012; published 9 Feb 2012

$$\left|A_2(z)\right|^2 = \frac{1}{4} + \frac{1}{4}\cos^2\left(\bar{S}z\right) + \frac{1}{2}\cos\left(\bar{S}z\right)\cos\left[\left(\alpha_{22}+\alpha_{33}+C_{24}-\beta_2\right)z\right] + \frac{\alpha_{22}-\alpha_{33}}{4\bar{S}}\sin\left(\bar{S}z\right)\left\{\frac{\alpha_{22}-\alpha_{33}}{\bar{S}}\sin\left(\bar{S}z\right) - 2\sin\left[\left(\alpha_{22}+\alpha_{33}+C_{24}-\beta_2\right)z\right]\right\}, \tag{46}$$

$$\left|A_4(z)\right|^2 = \frac{1}{4} + \frac{1}{4}\cos^2\left(\bar{S}z\right) - \frac{1}{2}\cos\left(\bar{S}z\right)\cos\left[\left(\alpha_{22}+\alpha_{33}+C_{24}-\beta_2\right)z\right] + \frac{\alpha_{22}-\alpha_{33}}{4\bar{S}}\sin\left(\bar{S}z\right)\left\{\frac{\alpha_{22}-\alpha_{33}}{\bar{S}}\sin\left(\bar{S}z\right) + 2\sin\left[\left(\alpha_{22}+\alpha_{33}+C_{24}-\beta_2\right)z\right]\right\}, \tag{47}$$

and

$$\left|A_3(z)\right|^2 = \left|A_5(z)\right|^2 = \left(\frac{C_{32}}{\bar{S}}\right)^2 \sin^2\left(\bar{S}z\right). \tag{48}$$

Under the condition $\xi = C_{23}C_{32}/(\alpha_{22} - \alpha_{33})^2 << 1$ i.e. when the non-identical cores are well-isolated, $\bar{S} \cong (\alpha_{22} - \alpha_{33})[1 + 2\xi\,]$ for $\alpha_{22} > \alpha_{33}$ and $\bar{S} \cong -(\alpha_{22} - \alpha_{33})[1 + 2\xi\,]$ for $\alpha_{22} < \alpha_{33}$. In this case, Eq. (46) can be written as

$$\begin{aligned}\left|A_2(z)\right|^2 &= \cos^2\left[\left(\alpha_{22}-\alpha_{33}\right)\left(\frac{C_{24}}{\alpha_{22}-\alpha_{33}}+\xi\right)z\right] - \xi\sin\left(\bar{S}z\right)\left\{\sin\left(\bar{S}z\right) \mp \sin\left[\left(\alpha_{22}+\alpha_{33}+C_{24}-\beta_2\right)z\right]\right\} \\ &\cong \cos^2\left[\left(\alpha_{22}-\alpha_{33}\right)\left(\frac{C_{24}}{\alpha_{22}-\alpha_{33}}+\xi\right)z\right]\end{aligned} \tag{49}$$

for small ξ and

$$\left|A_3(z)\right|^2 = \left|A_5(z)\right|^2 \cong 0. \tag{50}$$

It can be seen from Eq. (49) that although no power is coupled into dissimilar cores when ξ is small, the coupling dynamics within cores 2 and 4 depend on ξ and $C_{24}/(\alpha_{22} - \alpha_{33})$ which is typically a small value as well. In this case, ξ will not be negligible if such two terms are of the same order of magnitude. Equation (49) can be re-written as

$$\begin{aligned}&\left|A_2(z)\right|^2 = \cos^2\left(\frac{-j\left(\gamma_1-\gamma_3\right)}{2}z\right), \quad \left|A_4(z)\right|^2 = \sin^2\left(\frac{-j\left(\gamma_1-\gamma_3\right)}{2}z\right) \quad \text{for} \quad \Delta_2 > \Delta_3 \\ &\left|A_2(z)\right|^2 = \cos^2\left(\frac{-j\left(\gamma_1-\gamma_4\right)}{2}z\right), \quad \left|A_4(z)\right|^2 = \sin^2\left(\frac{-j\left(\gamma_1-\gamma_4\right)}{2}z\right) \quad \text{for} \quad \Delta_2 < \Delta_3\end{aligned} \tag{51}$$

yielding

$$\boldsymbol{\mathcal{L}}_{c2} = \begin{cases}\pi/\left|-j\left(\gamma_1-\gamma_3\right)\right| & \text{for} \quad \Delta_2 > \Delta_3 \\ \pi/\left|-j\left(\gamma_1-\gamma_4\right)\right| & \text{for} \quad \Delta_2 < \Delta_3\end{cases} \tag{52}$$

and

$$\left|A_2\left(\boldsymbol{\mathcal{L}}_{c1}\right)\right|^2 = 0. \tag{53}$$

From Eqs. (51)–(53), one can conclude that power from dissimilar core groups will not couple to each other as expected and the coupling between core 2 and 4 resemble those of a

#156104 - $15.00 USD Received 10 Oct 2011; revised 20 Dec 2011; accepted 1 Feb 2012; published 9 Feb 2012

homogeneous 2-core MCF. However, the generalized coupling length for this 4-core structure depends on the eigenvalue spread according to Eq. (52) and is different from that of a corresponding 2-core system in general. These eigenvalues and eigenmodes in turn depend on the overall geometry and index contrasts of the composite 4-core MCF. In other words, despite the fact that no power is coupled into cores 3 and 5, these dissimilar cores play a significant role in the coupling dynamics of cores 2 and 4. Alternatively, since $-j\gamma_p$ is the propagation constant for the p^{th} eigenmode, one can deduce that power transfer characteristics for composite waveguides depend on the differences between the propagation constants of the eigenmodes not the propagation constants of individual core modes. The use of eigenmodes for analyzing signal transmission in composite fiber structures has also been reported recently [39]. The analytical results can be generalized to MCFs with larger number of cores per group and hence coupling dynamics of heterogeneous MCFs studied in Section 3B can be understood under this framework. Finally, it can be noted that when ξ is so small such that $\xi << |C_{24}/(\alpha_{22} - \alpha_{33})| << 1$, $|A_2(z)|^2 \cong \cos^2(C_{24}z)$ i.e. the coupling dynamics truly approach to that of the corresponding 2-core system.

Acknowledgments

The authors would like to acknowledge the generous support of the Hong Kong Government General Research Fund (GRF) under project number PolyU 522009 and PolyU 519211.

#156104 - $15.00 USD Received 10 Oct 2011; revised 20 Dec 2011; accepted 1 Feb 2012; published 9 Feb 2012